

The Fall of the Youngest Planetary Nebula, Hen3-1357

Bruce Balick^{1*}, Martín A. Guerrero², Gerardo Ramos-Larios³

¹ Department of Astronomy, University of Washington, Seattle, WA 98195-1580, USA

² Instituto de Astrofísica de Andalucía (IAA-CSIC), Glorieta de la Astronomía S/N, 18008 Granada, Spain

³ Instituto de Astronomía y Meteorología, Universidad de Guadalajara, 44130 Guadalajara, Mexico

*Corresponding author: balick@uw.edu

Received xxxxxx

Accepted for publication xxxxxx

Published xxxxxx

Abstract

The Stingray Nebula, aka Hen3-1357, went undetected until 1990 when bright nebular lines and radio emission were unexpectedly discovered. We report changes in shape and rapid and secular decreases in its nebular emission-line fluxes based on well calibrated images obtained by the Hubble Space Telescope in 1996, 2000, and 2016. Hen3-1357 is now a “recombination nebula”.

Keywords: planetary nebulae: Planetary nebulae (1249), Post-asymptotic giant branch stars (2121), Ionization (2068)

1. Introduction

Planetary nebulae (“PNe”) consist of stellar gas ejected in winds from the surfaces of post Asymptotic Branch Giant (“AGB”) stars. The winds systematically expose deeper and much hotter interior stellar layers until stellar energetic ultraviolet (“UV”) begins to ionize the ejected gas. The PN radiates a rich, luminous, and readily detectable set of emission lines (e.g., δ) as electron recombinations with H^+ and He^+ and optical forbidden lines of N^+ , O^+ , O^{++} , S^+ , etc. These lines become increasingly visible by about a millennium after the winds begin as the central star shifts towards higher temperatures > 40 kK.

In extraordinary cases, of which the Stingray Nebula (aka Hen3–1357) is an outstanding example, the ionized nebula appears suddenly, almost like a miniature nova. An emission-line spectrum that is characteristic of PNe was initially and unexpectedly detected from Hen3-1357 in 1990 (Parthasarathy et al. 1993; hereafter “P+13”) and soon confirmed (Parthasarathy et al. 1995; Feibelman, 2015). Narrow-band images from the Hubble Space Telescope (HST) taken in 1992 and 1996 (Bobrowsky, 1994; hereafter “B94”, Bobrowsky et al. 1998) first revealed the compact nebula (largest angular radius $\theta = 0.''8$) (Figure 1). B94 identified Hen3-1357 as “the youngest PN”, a title wrested from LMC SMO 64 (Dopita & Meatheringham 1991). Judging from its present expansion speed, ~ 8.4 km s⁻¹ (Arhipova et al. 2013; hereafter “A+13”), size θ , and distance D , winds from its central star, SAO 244567, started forming the nebula $\sim 1000(D/\text{kpc})$ y prior to the onset of ionization (Reindl et al. 2014; hereafter “R+14”). This gestation time is characteristic of PNe (Schönberner et al. 2014). (Estimates of D/kpc range from 0.83 (Fresneau et al., 2007), 1.6 (R+14), 1.8 (A+13) and 1.63–4.92 (Otsuka et al. 2017; hereafter “O+17”).

This paper focusses on the actual changes in structure and surface brightness of Hen3-1357 over the last 20 years using archival images from the HST. We discuss history of Hen3-1357, information extracted from the downloaded images, and their interpretation in sections 2, 3, and 4, respectively.

2. History

Hen3-1357 has turned out to be the most rapidly evolving of all PNe. HST images (Figure 1) show how the surface brightness, detailed shape, and the nebular ionization state fluctuated dramatically between

1996 and 2106. Initial reports (Bobrowsky et al. 1998, A+13) suggested that low-ionization line ratios $[O\text{ I}]/H\beta$, $[O\text{ II}]/H\beta$, and $[N\text{ II}]/H\beta$ had doubled between 1992 and 2011, whereas the $[O\text{ III}]/H\beta$ ratio had decreased by the same factor. Secular changes in its radio Bremsstrahlung continuum strength (Harvey-Smith et al. 2018) have been comparable in magnitude to the flux changes of Balmer lines of H^+ , as expected. (Therefore, foreground extinction is not the cause of the rapid fading of Hen3-1357. This agrees well with the small interstellar reddening correction, $c(H\beta) = 0.083$, found by O+17)

The ionization rate of the nebula is governed by the evolution of ionizing UV photons from the central star. The nebular light traversal time is about a week, so the ionization rate of the gas responds very quickly to changes in the stellar UV flux and spectrum. The local recombination time scale per ion, $\approx 10^5 \text{ y}/(Z^2 n_e)$, is decades to centuries, depending on the local electron density, $n_e \text{ (cm}^{-3}\text{)}$ and the charge of the recombining ion Z . We have adopted a canonical value of $n_e \approx 10^4 \text{ cm}^{-3}$ (e.g., P+93, O+17).

Several detailed historical accounts of the evolution of the central star SAO 244567 exist (R+14, Schaefer & Edwards 2015; hereafter “BE15”, and Reindl et al. 2017; hereafter “R+17”). In brief, the B magnitude of SAO 244567 has faded steadily at a rate of 0.20 mag/y since nebular ionization began. The stellar surface temperature T_{eff} rose from 21 kK by 1980 to 38 kK in 1988, to a peak value of 60 kK in 2002 and then cooled to 50 kK in 2015. Its surface gravity, $\log g$, increased from 4.8 between 1988 and 2002 and rose to 6.0 in 2015 (Figure 4 in R+17) as the star initially contracted and then expanded.

The recent evolution of SAO 244567 is a conundrum. To explain its behavior, the Reindl collaboration group (R+14, R+17) proposed that the star underwent a disruptive late thermal pulse and is now returning to the top of the “Asymptotic Giant Branch” (AGB) in the canonical Hertzsprung-Russel Diagram. However, this interpretation is not without substantial problems (13). If SAO 244567 follows the usual post-AGB tracks in the H-R diagram (15) then the time scales of its rapid changes require a stellar mass of at least 0.7 solar masses (M_{\odot}). However, its current location on the H-R diagram requires a stellar mass $< 0.53 M_{\odot}$ (BE15, R+14). Moreover, these and other evolutionary scenarios each have fundamental shortcomings (BE15), not the least of which is that the very rapid in luminosity and temperature changes of SAO 244567 are a poor fit to model evolution trajectories following thermal pulsations.

3. Archival Results

The HST images used here were downloaded in calibrated form from the Hubble Legacy Archive¹. They were originally obtained using two telescope cameras, WFPC2 and WFC3, each with different filters and detectors. Accordingly, we divided the count rates per pixel by the total throughout efficiencies for each camera-filter combination and verified the accuracy of their relative intensities to $\pm 10\%$ using non-variable field stars. The images were spatially registered using the central star or its nearby fainter and cooler binary companion.

HST images of Hen3-1357 in the emission lines of $[O\text{ III}]$, $[N\text{ II}]$, and $H\alpha$ are shown in Figure 2 in pairs of rows from top to bottom, as indicated. The peak count rate and other vital descriptive information is shown at the bottom of each panel. Very substantial changes appear in the peak count rates and nebular shapes from filter to filter and epoch to epoch. The ratios of the peak count rates between 1996 and 2016 changed by -50% , $+7\%$, and -33% for the $H\alpha$, $[N\text{ II}]$, and $[O\text{ III}]$ images, respectively. The changes in a few individual features are shown by white arrows and numbers within the top right panels for each pair of rows.

¹ Based on observations made with the NASA/ESA Hubble Space Telescope, and obtained from the Hubble Legacy Archive, which is a collaboration between the Space Telescope Science Institute (STScI/NASA), the Space Telescope European Coordinating Facility (ST-ECF/ESA) and the Canadian Astronomy Data Centre (CADC/NRC/CSA).

The most dramatic changes are found in the [O III] images, as expected since its recombination rate is 4 times higher at constant density. We see that the two lobes at 5 and 11 o'clock vanish entirely, whereas the lobe pairs at 2 and 8 o'clock fade more slowly or, in some zones, brighten by $\sim 50\%$ at the lobe tips in $H\alpha$ and [N II]. In addition, four bright arcs at the interstices of the lobes seen in the first two [N II] panels all but vanish in the 2016. The color panels in Figure 2 highlight some subtle but significant changes in the size and orientation of the central ellipse.

Table 1a. Detected Fluxes of Narrowband Images of Hen3-1357

Integrated Line Fluxes (10^{-12} erg cm^{-2} s^{-1})	$H\beta^a$ 486 nm	[O III] ^a 501 nm	He I 587 nm	[O I] 630 nm	$H\alpha$ 656 nm	[N II] 658 nm	[S II] 672+3 nm
Camera Filter Name	F487N	F502N	F588N	F631N	F656N	F658N	F673N
1996 (WFPC2)	1.65	12.1	0.31	0.28	5.40	1.76	0.22
2016 (WFC3)	0.67	2.45			1.99	1.03	0.21
Flux ratio 2016/1996	0.41	0.20			0.37	0.59	0.96

Table 1b. Flux Ratios of Image Total Fluxes to $H\beta = 1$

Line Fluxes/ $H\beta$	($H\beta=1$)	[O III]/ $H\beta$	He I/ $H\beta$	[O I]/ $H\beta$	$H\alpha/H\beta$	[N II]/ $H\beta$	[S II]/ $H\beta$
1996 (WFPC2)	(1)	7.3	0.19	0.17	3.3	1.1	0.13
2016 (WFC3)	(1)	3.7			3.0	1.5	0.31
2006 from (O+17)	(1)	4.2	0.15	1.6	(3.0 ^b)	1.2	0.18

a. Extinction-corrected ($H\beta$, [O III]) fluxes were (1.9×10^{-11} , 2.2×10^{-9}) erg cm^{-2} s^{-1} in 1990 and (5.8×10^{-11} , 6.4×10^{-10}) erg cm^{-2} s^{-1} in 1992 (B94).

b. Estimated (O+17)

Changes in the summed image fluxes within the filter set are presented in Table 1a. The image intensities were converted to energy fluxes, erg cm^{-2} s^{-1} pixel⁻¹ and summed over the nebular image. Table 1b shows the ratios of total image fluxes relative to $H\beta (= 1)$ from the 1996 images (top row) and 2016 images (middle row). Spectrophotometric ratios for 2006 from O+17 appear in the bottom row. The ratios of total line fluxes of [N II]/ $H\beta$ and [S II]/ $H\beta$ increased while [O III]/ $H\beta$ decreased by 50%.

4. Discussion

To understand the changes in nebular brightness, color, and shape, first recall that the recombination rate per ion scales as $(Z^2 n_e)^{-1}$. The flux of the [O III] dropped line by a factor of 900 since 1990 owing to the relatively rapid recombination rate of O^{++} ions. The $H\beta$ flux dropped by much smaller factor of 29 (not 900/4) during the same interval. We ascribe this discrepancy to somewhat higher densities in the O^{++} ionization volume than the H^+ volume. On the other hand, the fluxes of the N^+ and S^+ increased between 1996 and 2016. The recombination of N^{++} and S^{++} enhanced the ionization fraction of N^+ and S^+ faster than the recombination rates of these ions. Therefore, it is clear that Hen3-1357 is presently a “recombination nebula” in which the volumetric rates of ionization and recombination are out of balance.

Let us assume that the observed decrease of the [O III] flux since 1990 dropped exponentially and that this decrease was dominated by recombinations in the O^{++} zone at a temperature, $T_e = 10^4$ K. The resulting O^{++} recombination time scale is 3.8y. This implies a mean electron density in the O^{++} zone of 4×10^4 cm^{-3} during that time. The recombination rate and the volume emissivity of the [O III] line scale as $n(O^{++}) n_e$, so the total [O III] flux is weighted towards zones of high density and fastest recombinations. This estimate for n_e is consistent with the higher densities of $> 2 \times 10^4$ cm^{-3} found from the ratios of multiply ionized forbidden lines (O+17, see Table 4).

One pair of faint outer lobes and their nearby environs became neutral and dark between 1996 and 2016 (Figure 2). The orthogonal pair of lobes all but vanished in zones traced by O^{++} lines even as their outer tips brightened slightly. This implies that the ionization histories of the two pairs of lobes may have

followed very different paths after the onset of ionization. The reasons are not clear. Perhaps the cone-like shapes of the lobes at 2 and 8 o’clock hints that they were shaped by collimated flows, at least initially. If so, an invisible stellar jet may still collisionally heat the tips of the lobes.

There are other PNe whose central stars have behaved similarly to SAO 244567, such as HDW 11, K 2–2, GD 561, PHL 932, and DeHt5. Most notably, Hen3-1357 can be compared to HuBi 1, another PN that is actively recombining after its central star dimmed by ~ 10 mag (a factor of 10^4) in the last 50y (Guerrero et al., 2018). The time-evolution of fluxes of HuBi 1’s respective emission lines behave similarly when the ratios of their current recombination time scales, ~ 5 , and structural complexities are considered. However, Hen 3–1357 is the only PN of its type for which the brightness its central star was monitored long before the star rapidly faded and its nebula appeared (BE15). This connection between its history and its future behavior makes the case of Hen3-1357 a special and important one.

In summary, SAO 244567 seems to have undergone a rapid shrinking with a rapid decrease in its ionizing luminosity in the early 1980s. Quoting Parthasarathy et al. (1995), “[The present] results suggest in the central star the nuclear fuel is almost extinct.” The ionization of its 1000-y-old PN, Hen31357 fell dramatically as a consequence (thus the “fall” of Hen3–1357). Recombinations now dominate the ionization state of the nebula. The ionization will slowly recover if SAO 244567 finds its way onto back to a standard post-AGB track, perhaps in a few decades. In this case the resurgence of optical emission lines may be accompanied by the emergence of a new bright core of hydrogen depleted, metal-rich inner gas, as was the case in Abell 30 and 78. Then the youngest PN will have risen again.

Acknowledgements

Acknowledgements: MAG acknowledges financial support by grant PGC2018-102184-B-I00, co-funded with FEDER funds, and from the State Agency for Research of the Spanish Ministerio de Ciencia, Innovacion y Universidades through the “Center of Excellence Severo Ochoa” award for the Instituto de Astrofísica de Andalucía (SEV-2017-0709).

Facility HST (WFPC2, WFC3)

References

- Arhipova, V.P., Ikonnikova, N.P., et al. 2013AstL...39..201A
 Bobrowsky, M. 1994ApJ...426L..47B
 Bobrowsky, M., Sahu, K.C., et al. 1998Natur.392..469B
 Dopita, M.A. and Meatheringham, S.J. 1991ApJ...374L..21D
 Feibelman, W.A. 1995ApJ...443..245F
 Fresneau, A., Vaughn, A.E., and Argyle, R.R. 2007A&A...469.1221F
 Guerrero, M., Fang, X., et al., 2018NatAs...2..784G
 Harvey-Smith, L., Hardwick, J. A., et al., 2018MNRAS.479.1842H
 Miller Bertolami, M.M., 2016A&A...588A..25M
 Otsuka, M., Parthasarathy, M., et al. 2017ApJ...838...71O
 Parthasarathy, M., Garcia-Lario, P., et al. 1993A&A...267L..19P
 Parthasarathy, M., Garcia-Lario, P., et al. 1995A&A...300L..25P
 Reindl, N., Rauch, T., et al. 2014A&A...565A..40R
 Reindl, N., Rauch, T., et al. 2017MNRAS.464L..51R
 Schaefer, B.E. & Edwards, Z. 2015ApJ...812..133S
 Schönberner, D., Jacob R., et al. 2014AN....335..378S

Figures

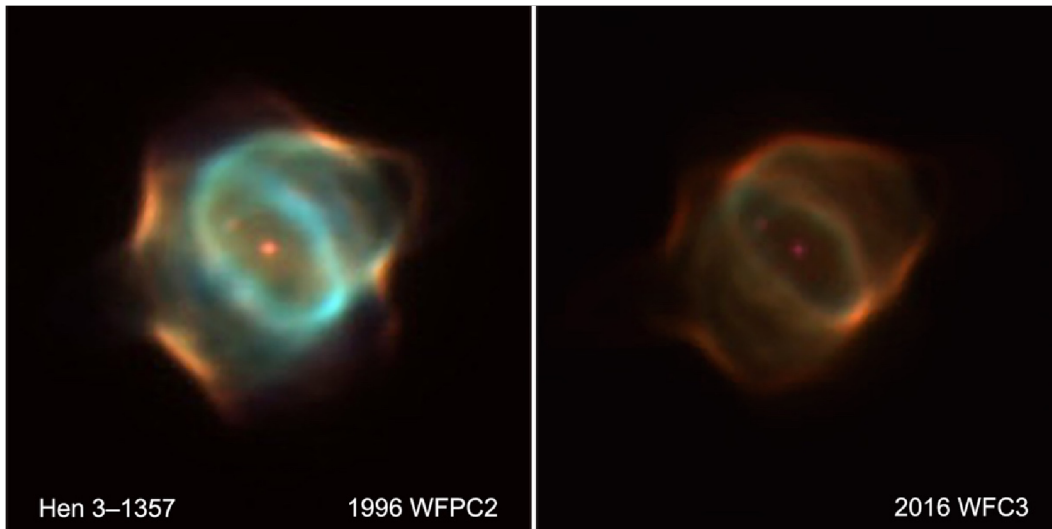


Figure 1. Hubble Telescope images of Hen3-1357 taken over 20 years. These reveal the changes in surface brightness in the emission lines of N^+ (red), H^+ (green) and O^{++} (blue).

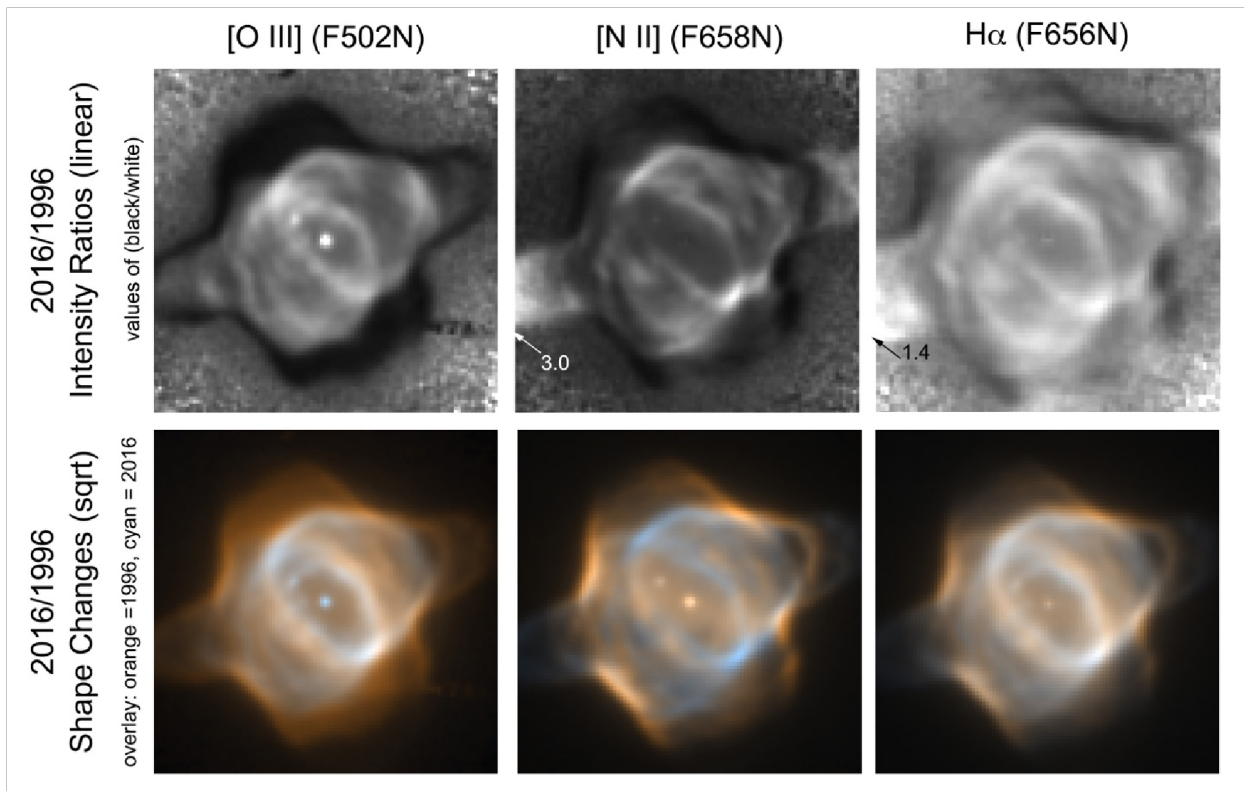


Figure 2. A montage of complementary and repeated narrowband imaging observations of Hen31357 in 1996, 2000, and 2016. The emission line and corresponding filter are listed across the top. Top row (left to right): two-epoch image ratios normalized to their respective peak ratios of 0.5, 2.0, and 0.6, (white = 0.5 corresponds to a brightness decrease of 50%; black is zero). Exceptional values are indicated by arrows. The bottom row shows changes in the structure over 20 y as two-color overlays, where the peak pixel is always unity.